Journal of Molecular Structure 1277 (2023) 134831

Contents lists available at ScienceDirect

Journal of Molecular Structure

journal homepage: www.elsevier.com/locate/molstr

Comparison of bacteria in different metabolic states by micro-Raman spectroscopy

Haodong Shen[a,b,c], Petra Rösch[a,b,*], Lara Thieme[d,e], Mathias W. Pletz[d], Jürgen Popp[a,b,c]

[a] Institute of Physical Chemistry, Friedrich Schiller University Jena, Helmholtzweg 4, Jena D-07743, Germany
[b] InfectoGnostics Research Campus Jena, Philosophenweg 7, Jena D-07743, Germany
[c] Leibniz Institute of Photonic Technology Jena - Member of the Research Alliance "Leibniz Health Technologies", Albert-Einstein-Str. 9, Jena D-07745, Germany
[d] Jena University Hospital, Institute of Infectious Diseases and Infection Control, Friedrich-Schiller-University Jena, Am Klinikum 1, Jena 07747, Germany
[e] Leibniz Center for Photonics in Infection Research, Jena University Hospital, Friedrich Schiller University Jena, Jena 07747, Germany

ARTICLE INFO

Article history:
Received 21 September 2022
Revised 29 November 2022
Accepted 19 December 2022
Available online 20 December 2022

Keywords:
Biofilm
Micro-Raman spectroscopy
Planktonic
Metabolic states

ABSTRACT

It was shown that several metabolic states of bacteria with various characteristics such as chemical composition participate in the formation of biofilms. To study the connections and differences among different bacterial metabolic states, five species of bacteria in exponential phase, stationary phase and biofilm have been compared and investigated by micro-Raman spectroscopy. The spectral differences between different metabolic states showed that the chemical composition varied among those metabolic states. Moreover, as can be shown by the spectral differences and principal components (PCs), different species and strains of bacteria behave differently. Furthermore, a principal component analysis (PCA) combined with support vector machines (SVM) was applied to distinguish species of bacteria within the same metabolic states. Our study provides valuable data for the comparison of bacteria between different metabolic states utilizing micro-Raman spectroscopy in combination with chemometrics models.

1. Introduction

In batch culture, free-living, planktonic bacteria usually follow a typical growth pattern with distinct growth phases, i.e. the lag, exponential (log) and stationary phase [1]. During the initial lag phase, bacterial cells adjust to the environment by upregulating the cellular processes required for proliferation [2]. Independent from nutrient availabilities, the bacterial population will start to grow in a logarithmic fashion in the exponential growth phase, quickly accumulating its biomass [2]. The resulting waste products limit further growth and lead to an equilibrium of alive and dead cells called the stationary phase [3].

Besides the planktonic lifestyle, bacteria can aggregate and embed themselves into a self-produced matrix of extracellular polymeric substances (EPS), forming microbial communities called biofilms. Normally biofilms form when non-optimal conditions like e.g. starvation occur [4]. During biofilm formation, starting with planktonic cells, bacterial cells attach irreversibly to surfaces when triggered by environmental elements, such as temperature, growth media, and pH [5]. After the attachment, the sessile bacteria secrete EPS and gradually constitute a mature biofilm. In the end, the biofilm will break and release once more planktonic cells [6]. These planktonic cells may start a new round of biofilm formation somewhere else. Sessile bacteria in biofilms exhibit a higher tolerance to antimicrobials than planktonic cells. This antibiotic tolerance is not conferred by classical genetic resistance determinants and is lost when bacteria transfer back into the planktonic phase. Biofilm-embedded cells show different levels of metabolic activity, with slow-growing subpopulations such as persister cells and some faster-growing, exponential-phase-like cells responsible for bacterial dispersal. Overall, biofilm-embedded cells resemble the metabolic activity of stationary phase planktonic cells [7].

A multitude of strategies have been applied to compare different metabolic states in bacteria. Genomics and proteomics have been widely used to explore the differences and connections between different metabolic states [8–11]. Whiteley et al. demonstrated that only 1% of genes expressed differently in biofilms and planktonic bacteria when assessed by DNA microarrays despite huge differences between these two metabolic states [12]. Sauer et al. demonstrated that several proteins in mature biofilm cells of *P. aeruginosa* were differentially expressed, with protein expression

* Corresponding author at: Institute of Physical Chemistry, Friedrich Schiller University Jena, Helmholtzweg 4, Jena D-07743, Germany.
E-mail address: petra.roesch@uni-jena.de (P. Rösch).

https://doi.org/10.1016/j.molstruc.2022.134831

patterns showing the great variation compared to those of planktonic cells [13]. However, the genes and proteins expressed in different metabolic states are not functionally irreplaceable or reproducibly, therefore it may be difficult to derive a therapeutic and diagnostic value from these results [10]. To address this problem, matrix assisted laser desorption ionization - time of flight (MALDI-TOF) mass spectrometry is also used to analyze protein in exponential phase, stationary phase and biofilms. The proteomic patterns showed different protein composition between biofilms and planktonic cells which indicate a unique lifestyle for *A. baumannii* biofilms compared to planktonic cells. This could allow the identification of proteins with possible character in biofilm formation and maintenance [14].

Vibrational spectroscopy such as Raman spectroscopy is a reagent-free approach where chemical dyes or labels for identification are not necessary. The characteristic of Raman spectroscopy is that it is a non-invasive, rapid, and accurate analytical method that offers a potential approach to identify bacteria [15]. It will not destroy the sample like mass spectrometry and may leave the sample for further analysis. Transformation between the different growth phases of planktonic cells as well as the switch to the biofilm lifestyle is accompanied by chemical composition variances, which can also be depicted by micro-Raman spectroscopy, since it is a phenotypic approach. The respective Raman signals represent the variance in the chemical compositions of the bacteria such as protein, DNA, RNA, polysaccharides and lipids [16–19]. Raman spectroscopy has already been applied in exploring different metabolic states and biofilms [20–23]. Escoriza et al. reported that the Raman signals of nucleic acids in *S. epidermidis* and *E. coli* decrease after the metabolic state of the bacteria changed from the exponential phase to the stationary phase [20]. A study by Kusić et al. described the chemical variances between planktonic cells and sessile cells in biofilms by applying micro-Raman spectroscopy with an excitation wavelength of 532 nm. Here, chemometric models were also established for the differentiation of sessile cells and planktonic cells [21]. However, in the described studies, a comparison of planktonic cells in different growth phases, i.e. exponential phase and stationary phase, with sessile cells in biofilms has not been elaborated. It is expected that sessile cells in biofilms are more similar to bacteria in the stationary phase than in the exponential phase, since the formation of persisters is a general stress response [4]. The similarities and dissimilarities between planktonic cells and sessile cells in biofilms are important to understand the formation and metabolism of biofilm. Furthermore, the chemical differences which are represented by the micro-Raman spectra may provide a unique description for cells at the corresponding metabolic states.

In this study, micro-Raman spectroscopy has been applied to evaluate the chemical compositions of single bacterial cells in the exponential phase, stationary phase, and single sessile cells in biofilms. To show the relation and distinction between different lifestyles, Raman spectra of the bacterial species *Pseudomonas aeruginosa, Staphylococcus aureus, Staphylococcus epidermidis, Enterococcus faecium* and *Enterococcus faecalis* obtained from single cells in three metabolic states were compared. And for the first time, the Raman spectra between single cells in exponential phase and sessile cells in biofilms are considered. Together with the comparison between single cells in the stationary phase and sessile cells in biofilm, we show how the chemical composition differs between those lifestyles as well as the similarities between them. Furthermore, a principal component analysis (PCA) was applied to understand the differences and relations between different metabolic states, especially between the single cells in the exponential phase and sessile cells in the biofilm. To further demonstrate the variances between these metabolic states, statistical models combined with PCA and support vector machines (SVM) were performed on spectra of bacteria in different metabolic states and all bacterial spectra.

2. Material and methods

2.1. Bacterial strains and media

The following ten strains were examined in the current study: *S. aureus* DSM20231, *S. aureus* BK31397, *S. epidermidis* RP62A, *S. epidermidis* VA78203, *E. faecium* UK005, *E. faecium* BK24498, *E. faecalis* DSM20478, *E. faecalis* VA245, *P. aeruginosa* DSM22644 and *P. aeruginosa* VA36580. The strains, *S. aureus* DSM20231, *S. epidermidis* RP62A, *E. faecalis* DSM20478 and *P. aeruginosa* DSM22644 were supplied from the German Collection of Microorganisms and Cell Cultures (Leibniz Institute DSMZ, Braunschweig, Germany). The others were obtained from the Institute of Medical Microbiology, Jena University Hospital. For the convenience of comparison and explanation, we assign *E. faecium* UK005 together with *S. aureus* DSM20231, *S. epidermidis* RP62A, *E. faecalis* DSM20478 and *P. aeruginosa* DSM22644 into the DSMZ group, the other five strains as a clinical group. For long storage, all bacteria were kept at -80 °C. To obtain bacterial colonies, bacteria were inoculated on LB agar (Carl Roth, X969.1) and incubated at 37 °C overnight. Liquid cultures were prepared with 3 g/L tryptic soy broth (Sigma Aldrich, 1054590500) supplemented with 2 g/L glucose (Sigma Aldrich, G8270-1KG).

2.2. Drip flow reactor (DFR)

To model the environments where biofilms originally grow such as catheters, lungs with cystic fibrosis and the oral cavity, a drip flow biofilm reactor was applied here [24]. The in-house-made biofilm reactor contains four parallel chambers with vented lids on the cover and in each chamber CaF_2 slides were inserted in the center. The media inflow into the chamber was realized through a cap on the cover and the outflow into a waste glass bottle. In batch mode, the chambers will stay horizontal. While working in flow mode, the reactor was maintained at 10 ° to the horizontal line. The media was pumped by a peristaltic pump (Heidolph Instruments GmbH, Schwabach, Germany) and a constant flow speed was ensured.

2.3. Planktonic cell preparation

The bacteria were grown in batch culture in the liquid media at 37 °C with 120 rpm shaking. During the growing process aliquots were taken from the suspension and the number of bacteria was estimated by measuring the optical density (OD) at a wavelength of 600 nm every hour. The cells in exponential phase were taken from the first OD measurement indicating that the bacterial cells enter the exponential phase, the cells in the stationary phase were selected after 24 h. An example is shown in Fig. S1 (supporting information). For Raman measurements bacterial aliquots were taken from the exponential and the stationary phase, respectively. The samples were washed by centrifugation at 5000 g and 4 °C for 5 min. The supernatant was discarded, and the pellet was suspended in sterile distilled water. After the washing process was performed three times, the sample was pipetted onto a nickel slide and dried at room temperature. The dried example of bacteria in exponential phase (B) and stationary phase (C) are shown in microscopic images in Fig. S1.

2.4. Sessile cells in biofilm preparation

Bacteria were multiplied at 37 °C with 120 rpm shaking in liquid media overnight. Then the DFR was established in the batch

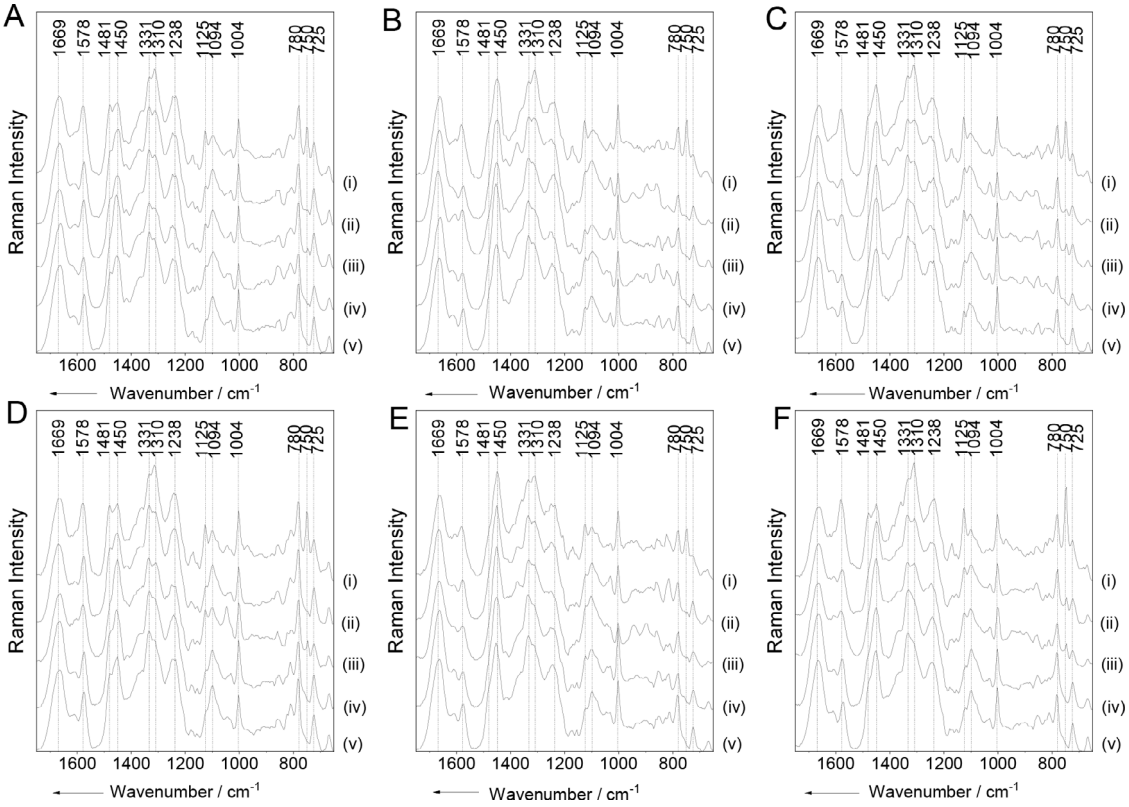

Fig. 1. Mean Raman spectra of bacteria for the DSMZ group (A–C), namely *P. aeruginosa* DSM 22644 (i), *S. aureus* DSM 20231 (ii), *S. epidermidis* RP62A (iii), *E. faecium* UK005 (iv) and *E. faecalis* DSM 20478 (v), and the clinical group (D-F), namely *P. aeruginosa* VA36580 (i), *S. aureus* BK31397 (ii), *S. epidermidis* VA78203 (iii), *E. faecium* BK24498 (iv) and *E. faecalis* VA245 (v), at exponential phase (A and D), stationary phase (B and E) and sessile cells (C and F) in biofilms.

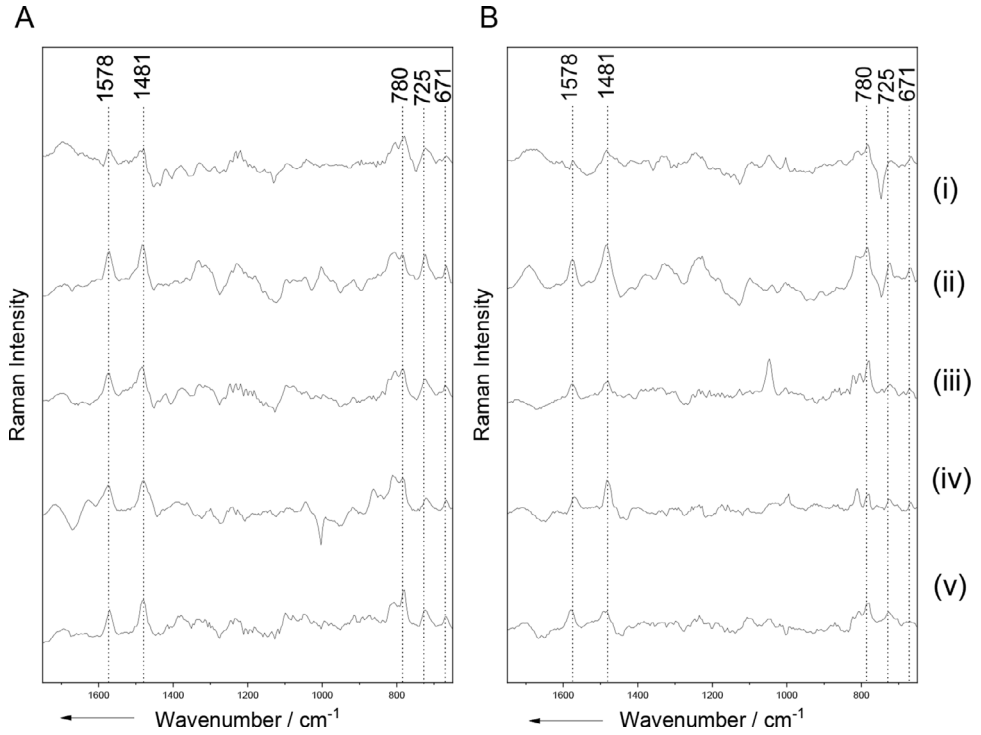

Fig. 2. Raman difference spectra between single bacteria in the exponential phase and sessile cells in biofilms of (A) the DSMZ group and (B) the clinical group. *P. aeruginosa* (i), *S. aureus* (ii), *S. epidermidis* (iii), *E. faecium* (iv) and *E. faecalis* (v).

mode: With clipped outflow pipes, 15 mL of fresh liquid media with 1 mL of the bacterial suspension was transferred into each of the DFR chambers at 37 °C and cultivated for 16 h in batch mode. After that, DFR started to work in flow mode: the flow speed was set to 12 mL/h and then the media flowed through the chamber. After 72 h, the CaF_2 slides were taken out and carefully rinsed with sterile distilled water. The biofilms on CaF_2 slides were removed carefully with an inoculation loop and then moved onto nickel foil and dried at room temperature. The microscope image of a dried example of sessile cells in a biofilm (D) is shown in Fig. S1.

2.5. Instrument setup

The Raman spectra of bacteria in exponential phase, stationary phase and biofilms were obtained with a Raman microscope (BioParticleExplorer, rap.ID Particle Systems GmbH, Berlin, Germany). The wavelength of the incident light was 532 nm from a solid-state frequency-doubled Nd:YAG laser source (LCM-S-111-NNP25; Laser-export Co. Ltd., Moscow, Russia) with a laser power of about 10 mW. An Olympus MPL-FLN-BD 100 × objective (Olympus Corporation, Tokyo, Japan) focused the Raman excitation light onto the sample with a spot size of around 1 μm. After removal of the Rayleigh scattering, the scattered Raman light was diffracted with a single-stage monochromator (HE 532; Horiba Jobin Yvon, Munich, Germany) equipped with a 920 lines mm^{-1} grating and detected by a thermoelectrically cooled charge-coupled device (CCD) camera (DV401-BV; Andor Technology, Belfast, Northern Ireland) with a spectral resolution of 8 cm^{-1}. To record a single spectrum, a single bacterial cell was measured with 10 s integration time and 10% of the laser output power. While measuring biofilms, a single sessile cell was selected and measured. Raman spectra of planktonic cells in exponential phase and stationary phase as well as sessile cells in biofilms for each strain were obtained from three independently grown and measured replicates. During the measurement, prepared bacterial replicates were moved to different sample holders, replicates were measured one by one. From each replicate, around 50 Raman spectra each from one single bacterial cell were obtained.

2.6. Data analysis

A classification procedure was performed in this study. All preprocessing was done using a Raman analysis App (Leibniz IPHT Ramanmetrix^{TM}). Raw Raman spectra have first been through despiking to remove cosmic spikes, then the wavenumber was calibrated using Raman spectra of acetaminophen measured at the same day as the reference. Next, to remove the spectral background, a method based on the SNIP clipping algorithm was applied [25]. Finally, all spectra were vector-normalized. Besides, the highlighted wavenumber region between 1750 and 650 cm^{-1}, which covers the fingerprint for most chemical components was used. Using this spectral region, the performance of the chemometric analysis greatly improved. Pre-processed data were used as input for principal component analysis (PCA). To classify the data, a support vector machines (SVM) model with radial basis kernels [26] was created and estimated using the leave-one-batch-out-cross-validation (LOBOCV) method [27]. The number of principal component variables was optimized by finding the best cross-validation on the training data based on the mean sensitivity of the SVM.

3. Results and discussion

The primary goal of this study is to investigate dissimilarities as well as similarities between sessile cells in biofilms and bacteria in different growth phases, thus a single bacterium was measured for each spectrum. Especially, for sessile cells in biofilms, every individual bacterium was localized, and the laser focused on it (Fig. S1D).

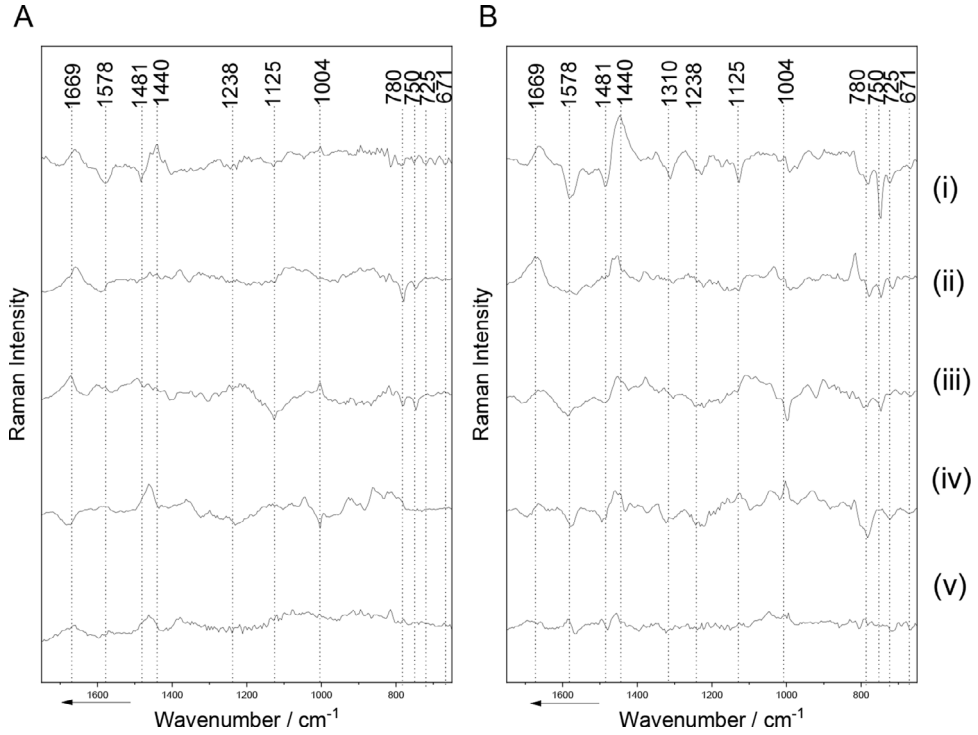

Fig. 3. Raman difference spectra between single bacteria in the stationary phase and sessile cells in biofilms of (A) the DSMZ group and (B) the clinical group. *P. aeruginosa* (i), *S. aureus* (ii), *S. epidermidis* (iii), *E. faecium* (iv) and *E. faecalis* (v).

3.1. Mean spectra

The mean Raman spectra of each species (i-v) in the exponential phase (A and D), the stationary phase (B and E), and the biofilms (C and F) are shown in Fig. 1. While measuring a single bacterium with an excitation wavelength of 532 nm, the whole biochemical information of this cell was collected in the respective Raman spectrum. Although there are superimposed signals originating from different contributions in the same Raman signal, we can still identify the composition of the cell through band assignments. Considering the CH_2 and CH_3 groups present in all macromolecules, the band centered at 1450 cm^{-1} shows the CH_2 and CH_3 deformation vibration modes [28,29]. At 1669 cm^{-1} and 1238 cm^{-1}, amide I and amide III signals representing protein were found, respectively [[30,31]. The ring breathing vibration modes of phenylalanine and tryptophan introduce a band at 1004 cm^{-1} [18,30]. The Raman bands appearing at 1578, 1481, 1331, 780 and 725 cm^{-1} are from nucleic acids [28,30]. The symmetric stretching vibrations of C-O-C glycosidic linkage are located at 1125 cm^{-1} [28], whereas the asymmetric stretching vibrations of C-O-C glycosidic linkage and C-C skeletal bond are observed at 1097 cm^{-1} [32]. These two bands can be assigned to polysaccharides. In the mean spectra of both strains, despite the metabolic states, *P. aeruginosa* exhibits higher signals at 1578, 1310, 1125 and 750 cm^{-1} which may be due to the existence of cytochrome [33,34].

3.2. Spectral differences

To investigate the dissimilarities as well as similarities of bacteria in different metabolic states, we calculated the differences of the mean Raman spectra between the exponential phase and the biofilms as well as the stationary phase and biofilms. Fig. 2 shows

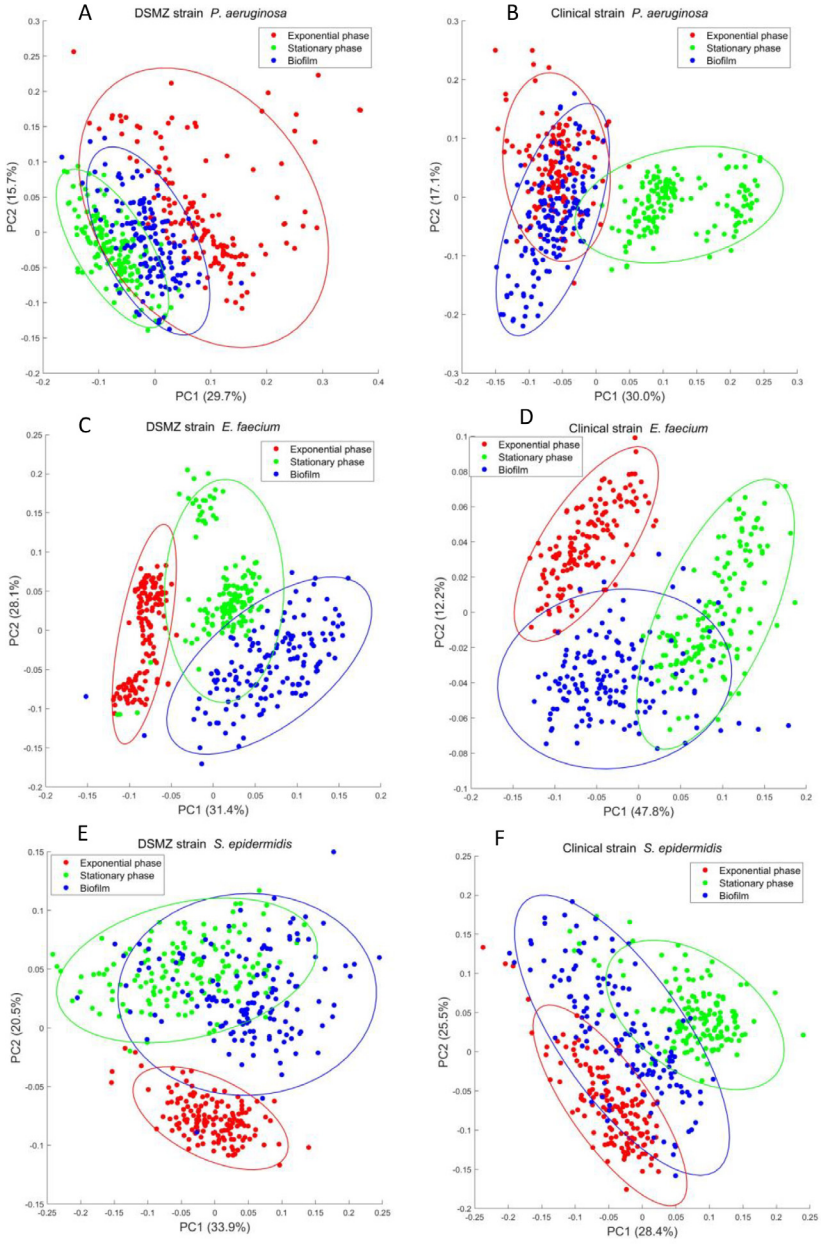

Fig. 4. Principal component analysis (PCA) scatter plot using the PC1 and PC2 values of Raman spectra for different metabolic states within the same species. (A) DSMZ strain and (B) clinical strain of *P. aeruginosa*, (C) DSMZ strain and (D) clinical strain of *E. faecium*, (E) DSMZ strain and (F) clinical strain of *S. epidermidis*, whereby each cross represents one spectrum and each ellipse correspond to 95% confidence regions for the PCA scores of each metabolic state.

the Raman difference spectra between single bacteria in the exponential phase and sessile cells in biofilms. Raman difference spectra from the DSMZ group as well as the clinical group show a higher relative intensity of the positive bands associated to nucleic acids (1578, 1481, 780, 725 and 671 cm^{-1}) in single cells from the exponential phase than sessile cells from biofilms.

Fig. 3 depicts the Raman difference spectra between single bacteria in the stationary phase and sessile cells in biofilms. For all the bacterial species in the clinical group (B), sessile cells in biofilms have more intense signals representing DNA and RNA (1578, 1481, 780, 725 and 671 cm^{-1}) than planktonic cells in the stationary phase. In both strains of *P. aeruginosa* (i), we observed sharp negative bands at 1578, 1310, 1125 and 750 cm^{-1} which can be attributed to cytochrome [33,34]. This shows that the Raman signals derived from cytochrome in sessile cells of *P. aeruginosa* are more intense than in the stationary phase. Moreover, in both difference spectra of *P. aeruginosa*, sessile cells in biofilms exhibit more intense signals from protein which can be observed by the negative bands at 1669, 1238 and 1004 cm^{-1}. However, planktonic cells in the stationary phase display an increased lipid signal at 1440 cm^{-1}.

The Raman spectral differences of single bacterial cells between different metabolic states show variations in chemical composition. Compared to planktonic cells in the exponential phase, the lower relative intensity of DNA signals may indicate that sessile cells in biofilms replicate slower. Here, *P. aeruginosa* is different from the other species: the relative intensity of the lipid signals in sessile cells in biofilms is lower than that of cells in the stationary phase. This may be due to the modification of *P. aeruginosa* membranes between sessile cells and planktonic cells characterized by Benamara et al [35]. Furthermore, the relative intensity of the Raman signals of cytochrome c in sessile cells is higher compared to planktonic cells in the stationary phase. This may be owing to the fact that cytochrome in *P. aeruginosa* supports the formation of biofilm and virulence [36]. Feng et al. also showed the increasing cytochrome amount during biofilm growth by Raman spectroscopy [37]. Moreover, from the mean Raman spectra, sessile cells in biofilms of *P. aeruginosa* are similar to bacterial cells in the exponential phase. To further illustrate this, PCA scatter plots using the first two principal components of Raman spectra for different metabolic states within each species are depicted in Fig. 4. In the PCA scatter plot of *P. aeruginosa* (A and B), bacterial cells in the exponential phase (red) stay close with sessile cells in biofilms (blue) for both the clinical strain and the DSMZ strain. However, in both the clinical strain and the DSMZ strain of *E. faecium* (C and D), in the PCA plot the bacterial cells in the stationary phase (green) are more similar to the sessile cells in biofilms (blue). For the DSMZ strain (E) of *S. epidermidis*, bacterial cells in the stationary phase (green) resembling more to the sessile cells in biofilms (blue), whereas this wasn't observed for the stationary phase and sessile cells in biofilms for the clinical strain (F) of *S. epidermidis.* For *E. faecalis* (Fig. S2) and *S. aureus* (Fig. S3), there is no unified conclusion either. Therefore, by the PCA plot of Raman spectra, the chemical composition of sessile cells in biofilms can be close to planktonic cells either in exponential phase or stationary phase. However, this depends on the species and strains of bacteria whose planktonic metabolic states are more comparable to sessile cells in biofilm.

Compared with well-documented methods such as genomics and proteomics in investigating the differences between planktonic cells and biofilms, instead of emphasizing the types of nucleic acid and protein expression [38,39], micro-Raman spectroscopy as a non-invasive and phenotypic approach is easier to monitor the change of the chemical compositions of the analyzed cells. In addition, Raman spectroscopy further provide a rapid and accurate method to classify between different species of bacteria.

Table 1
LOBOCV results for spectra of bacteria in different metabolic states and all bacterial spectra.

Sample	Classification (LOBOCV)		
	TP/CM*	Sensitivity / %	Specificity / %
Exponential phase			
S. epidermidis	185/299	61.9	97.4
S. aureus	260/299	87.0	89.0
E. faecium	233/295	79.0	98.5
E. faecalis	255/298	85.6	94.5
P. aeruginosa	294/298	98.7	98.6
Overall accuracy	1227/1489	82.4	
Stationary phase			
S. epidermidis	285/298	95.6	97.3
S. aureus	273/292	93.5	98.5
E. faecium	285/297	96.0	96.4
E. faecalis	268/298	89.9	99.2
P. aeruginosa	261/298	87.6	99.3
Overall accuracy	1372/1483	92.5	
Biofilm			
S. epidermidis	267/297	89.9	92.7
S. aureus	212/294	72.1	97.1
E. faecium	285/300	95.0	98.1
E. faecalis	269/292	92.1	97.8
P. aeruginosa	277/295	93.9	100
Overall accuracy	1310/1478	88.6	
All spectra			
S. epidermidis	699/894	78.2	95.9
S. aureus	735/885	83.1	93.9
E. faecium	730/892	81.8	95.6
E. faecalis	718/888	80.9	95.1
P. aeruginosa	861/891	96.6	99.7
Overall accuracy	3743/4450	84.1	

* TP = true positives, CM = all class members.

3.3. Classification

Similarities and dissimilarities of the mean Raman spectra between bacteria in the exponential and stationary phase as well as in the biofilm can be observed through the mean spectra differences, however it is impossible to correctly assign a single spectrum to species or growth states just by observing. Accordingly, with the advantage of chemometric techniques, it is practicable to differentiate the spectra in species level. Here, models were established to distinguish between Raman spectra of species in different growth states, another model combined all the spectra and aim to classify Raman spectra in of all species. PCA-SVM models for the differentiation between bacterial species was established and verified using the LOBOCV. For each species, two strains and three independent replicates for each strain are involved.

Table 1 shows the classification results for Raman spectra of bacteria in different metabolic states and all bacterial spectra. Bacteria at these different growth states were classified by a SVM at the species level. The overall accuracy for the exponential and stationary phase as well as the biofilm is 82.4%, 92.5% and 88.6%, respectively. The bacteria in the stationary phase and the biofilm have a higher classification accuracy whereas the bacteria in the exponential phase have the lowest accuracy. This might be because in the exponential phase bacteria have a higher physiological heterogeneity. In the classification model for all spectra, most Raman spectra were successfully classified, and the overall accuracy is 84.1%. Most of the misclassified spectra stay (shown in Table S4) within the same genus, for example, in the classification for spectra of *S. epidermidis*, 192 out of 195 misclassified spectra were assigned as *S. aureus*.

4. Conclusion

We compared bacterial cells from the exponential phase, stationary phase, and biofilms by micro-Raman spectroscopy which

can be used to find the variances among these metabolic states. It showed that the chemical composition of planktonic cells is different from sessile cells in biofilms, which enhanced the understanding of biofilm formation. Moreover, we saw that the cells of *P. aeruginosa* in exponential phase and biofilms are more related, while for other species this is not necessarily the case. Instead of a regular pattern, the chemical composition variances between different metabolic states depend on the strains and species. Our study further showed that micro-Raman spectroscopy combined with PCA-SVM, can nevertheless differentiate between species within the same metabolic state. It is also possible to classify the species of bacteria despite the metabolic states of bacteria. Those results showed that the chemical compositions of bacteria at different metabolic states are different, but also related to each other. The classifications of different species provide valuable data for further research of bacteria in different metabolic states. Moreover, biofilms are complex systems including different layers which may have various chemical compositions. It will be interesting to see in the future if the sessile cells from different layers in biofilm can be characterized separately.

Funding

This work was funded by the German Research Foundation (DFG) within the Jena School of Microbial Communication (JSMC).

Declaration of Competing Interest

The authors declare no competing interests.

CRediT authorship contribution statement

Haodong Shen: Conceptualization, Data curation, Investigation, Writing – original draft. **Petra Rösch:** Conceptualization, Supervision, Writing – review & editing. **Lara Thieme:** Conceptualization, Writing – review & editing. **Mathias W. Pletz:** Conceptualization, Resources, Supervision, Writing – review & editing. **Jürgen Popp:** Conceptualization, Resources, Supervision, Writing – review & editing.

Data availability

Data will be made available on request.

Acknowledgments

We would like to thank Darina Storozhuk and Dr. Oleg Ryabchykov for their parts in the development and support of the Ramanmetrix software. We appreciate Dr. Anita Hartung and Dr. Oliwia Makarewicz for collecting the clinical strains.

Supplementary materials

Supplementary material associated with this article can be found, in the online version, at doi:10.1016/j.molstruc.2022.134831.

References

[1] U. Wanner, T. Egli, Dynamics of microbial growth and cell composition in batch culture, FEMS Microbiol. Lett. 75 (1) (1990) 19–43.
[2] M.T. Madigan, J.M. Martinko, J. Parker, Brock Biology of Microorganisms, Pearson Prentice Hall, Upper Saddle River, New Jersey, 2006.
[3] R. Kolter, D.A. Siegele, A. Tormo, The stationary phase of the bacterial life cycle, Annu. Rev. Microbiol. 47 (1993) 855–875.
[4] J. Jaishankar, P. Srivastava, Molecular basis of stationary phase survival and applications, Front. Microbiol. 8 (2017) 2000.
[5] G. O'Toole, H.B. Kaplan, R. Kolter, Biofilm formation as microbial development, Annu. Rev. Microbiol. 54 (1) (2000) 49–79.
[6] D. Davies, Understanding biofilm resistance to antibacterial agents, Nat. Rev. Drug Discov. 2 (2) (2003) 114–122.
[7] T. Akerlund, K. Nordström, R. Bernander, Analysis of cell size and DNA content in exponentially growing and stationary-phase batch cultures of Escherichia coli, J. Bacteriol. 177 (23) (1995) 6791–6797.
[8] P. Stoodley, K. Sauer, D.G. Davies, J.W. Costerton, Biofilms as complex differentiated communities, Annu. Rev. Microbiol. 56 (2002) 187–209.
[9] A. Finelli, C.V. Gallant, K. Jarvi, L.L. Burrows, Use of in-biofilm expression technology to identify genes involved in Pseudomonas aeruginosa biofilm development, J. Bacteriol. 185 (9) (2003) 2700–2710.
[10] C.A. Fux, J.W. Costerton, P.S. Stewart, P. Stoodley, Survival strategies of infectious biofilms, Trends Microbiol. 13 (1) (2005) 34–40.
[11] W.L. Cochran, G.A. McFeters, P.S. Stewart, Reduced susceptibility of thin Pseudomonas aeruginosa biofilms to hydrogen peroxide and monochloramine, J. Appl. Microbiol. 88 (1) (2000) 22–30.
[12] M. Whiteley, M.G. Bangera, R.E. Bumgarner, M.R. Parsek, G.M. Teitzel, S. Lory, E. Greenberg, Gene expression in Pseudomonas aeruginosa biofilms, Nature 413 (6858) (2001) 860–864.
[13] K. Sauer, A.K. Camper, G.D. Ehrlich, J.W. Costerton, D.G. Davies, Pseudomonas aeruginosa displays multiple phenotypes during development as a biofilm, J. Bacteriol. 184 (4) (2002) 1140–1154.
[14] M.P. Cabral, N.C. Soares, J. Aranda, J.R. Parreira, C. Rumbo, M. Poza, J. Valle, V. Calamia, I. Lasa, G. Bou, Proteomic and functional analyses reveal a unique lifestyle for acinetobacter baumannii biofilms and a key role for histidine metabolism, J. Proteome Res. 10 (8) (2011) 3399–3417.
[15] C. Xie, J. Mace, M. Dinno, Y. Li, W. Tang, R. Newton, P. Gemperline, Identification of single bacterial cells in aqueous solution using confocal laser tweezers Raman spectroscopy, Anal. Chem. 77 (14) (2005) 4390–4397.
[16] R. Weiss, M. Palatinszky, M. Wagner, R. Niessner, M. Elsner, M. Seidel, N.P. Ivleva, Surface-enhanced Raman spectroscopy of microorganisms: limitations and applicability on the single-cell level, Analyst 144 (3) (2019) 943–953.
[17] C.S. Ho, N. Jean, C.A. Hogan, L. Blackmon, S.S. Jeffrey, M. Holodniy, N. Banaei, A.A.E. Saleh, S. Ermon, J. Dionne, Rapid identification of pathogenic bacteria using Raman spectroscopy and deep learning, Nat. Commun. 10 (1) (2019) 4927.
[18] X. Lu, H.M. Al-Qadiri, M. Lin, B.A. Rasco, Application of mid-infrared and Raman spectroscopy to the study of bacteria, Food Bioprocess Technol. 4 (6) (2011) 919–935.
[19] M.M. Hlaing, M. Dunn, P.R. Stoddart, S.L. McArthur, Raman spectroscopic identification of single bacterial cells at different stages of their lifecycle, Vib. Spectrosc. 86 (2016) 81–89.
[20] M.F. Escoriza, J.M. Vanbriesen, S. Stewart, J. Maier, Studying bacterial metabolic states using Raman spectroscopy, Appl. Spectrosc. 60 (9) (2006) 971–976.
[21] D. Kusić, B. Kampe, A. Ramoji, U. Neugebauer, P. Rösch, J. Popp, Raman spectroscopic differentiation of planktonic bacteria and biofilms, Anal. Bioanal. Chem. 407 (22) (2015) 6803–6813.
[22] N.P. Ivleva, M. Wagner, H. Horn, R. Niessner, C. Haisch, *In situ* surface-enhanced Raman scattering analysis of biofilm, Anal. Chem. 80 (22) (2008) 8538–8544.
[23] W.E. Huang, R.I. Griffiths, I.P. Thompson, M.J. Bailey, A.S. Whiteley, Raman microscopic analysis of single microbial cells, Anal. Chem. 76 (15) (2004) 4452–4458.
[24] D.M. Goeres, M.A. Hamilton, N.A. Beck, K. Buckingham-Meyer, J.D. Hilyard, L.R. Loetterle, L.A. Lorenz, D.K. Walker, P.S. Stewart, A method for growing a biofilm under low shear at the air-liquid interface using the drip flow biofilm reactor, Nat. Protoc. 4 (5) (2009) 783–788.
[25] C.G. Ryan, E. Clayton, W.L. Griffin, S.H. Sie, D.R. Cousens, SNIP, a statistics-sensitive background treatment for the quantitative analysis of PIXE spectra in geoscience applications, Nucl. Instrum. Methods Phys. Res. Sect. B 34 (3) (1988) 396–402.
[26] C. Cortes, V. Vapnik, Support-vector networks, Mach. Learn. 20 (3) (1995) 273–297.
[27] S. Guo, T. Bocklitz, U. Neugebauer, J. Popp, Common mistakes in cross-validating classification models, Anal. Methods 9 (30) (2017) 4410–4417.
[28] M. Harz, P. Rösch, K.D. Peschke, O. Ronneberger, H. Burkhardt, J. Popp, Micro-Raman spectroscopic identification of bacterial cells of the genus staphylococcus and dependence on their cultivation conditions, Analyst 130 (11) (2005) 1543–1550.
[29] M.L. Paret, S.K. Sharma, L.M. Green, A.M. Alvarez, Biochemical characterization of Gram-positive and Gram-negative plant-associated bacteria with micro-Raman spectroscopy, Appl. Spectrosc. 64 (4) (2010) 433–441.
[30] Z. Movasaghi, S. Rehman, I.U. Rehman, Raman spectroscopy of biological tissues, Appl. Spectrosc. Rev. 42 (5) (2007) 493–541.
[31] G. Rusciano, P. Capriglione, G. Pesce, P. Abete, V. Carnovale, A. Sasso, Raman spectroscopy as a new tool for early detection of bacteria in patients with cystic fibrosis, Laser Phys. Lett. 10 (7) (2013) 075603.
[32] A. Williams, H. Edwards, Fourier transform Raman spectroscopy of bacterial cell walls, J. Raman Spectrosc. 25 (7-8) (1994) 673–677.
[33] B. Lorenz, P. Rösch, J. Popp, Isolation matters-processing blood for Raman microspectroscopic identification of bacteria, Anal. Bioanal. Chem. 411 (21) (2019) 5445–5454.
[34] A. Walter, S. Erdmann, T. Bocklitz, E.M. Jung, N. Vogler, D. Akimov, B. Dietzek, P. Rösch, E. Kothe, J. Popp, Analysis of the cytochrome distribution via linear and nonlinear Raman spectroscopy, Analyst 135 (5) (2010) 908–917.
[35] H. Benamara, C. Rihouey, T. Jouenne, S. Alexandre, Impact of the biofilm mode of growth on the inner membrane phospholipid composition and lipid domains in Pseudomonas aeruginosa, Biochim. Biophys. Acta 1808 (1) (2011) 98–105.

[36] J. Jo, K.L. Cortez, W.C. Cornell, A. Price-Whelan, L.E. Dietrich, An orphan cbb3-type cytochrome oxidase subunit supports Pseudomonas aeruginosa biofilm growth and virulence, Elife 6 (2017) e30205.
[37] J. Feng, C. de la Fuente-Nunez, M.J. Trimble, J. Xu, R.E. Hancock, X. Lu, An *in situ* Raman spectroscopy-based microfluidic "lab-on-a-chip" platform for non-destructive and continuous characterization of Pseudomonas aeruginosa biofilms, Chem. Commun. 51 (43) (2015) 8966–8969 (Camb.).
[38] O. Dudin, J. Geiselmann, H. Ogasawara, A. Ishihama, S. Lacour, Repression of flagellar genes in exponential phase by CsgD and CpxR, two crucial modulators of Escherichia coli biofilm formation, J. Bacteriol. 196 (3) (2014) 707–715.
[39] T. Candela, A. Fagerlund, C. Buisson, N. Gilois, A.B. Kolsto, O.A. Okstad, S. Aymerich, C. Nielsen-Leroux, D. Lereclus, M. Gohar, CalY is a major virulence factor and a biofilm matrix protein, Mol. Microbiol. 111 (6) (2019) 1416–1429.